Explanations for anomalies of muon anomalous magnetic dipole moment, $b \to s\mu\bar{\mu}$, and radiative neutrino masses in a leptoquark model

Takaaki Nomura[1,*] and Hiroshi Okada[2,3,†]

[1]*College of Physics, Sichuan University, Chengdu 610065, China*
[2]*Asia Pacific Center for Theoretical Physics (APCTP)—Headquarters San 31,*
Hyoja-dong, Nam-gu, Pohang 790-784, Korea
[3]*Department of Physics, Pohang University of Science and Technology, Pohang 37673, Republic of Korea*

We propose a leptoquark model simultaneously to explain anomalies of muon anomalous magnetic dipole moment and $b \to s\mu\bar{\mu}$ in light of experimental reports very recently. Here, we satisfy several stringent constraints such as $\mu \to e\gamma$ and meson mixings. In addition, we find these leptoquarks also play an role in generating tiny neutrino masses at one-loop level without introducing any additional symmetries. We have numerical analysis and show how degrees our parameter space is restricted.

I. INTRODUCTION

The anomalous magnetic dipole moment of muon (muon $g - 2$) is precisely predicted in the Standard Model (SM) and the deviation from the prediction indicates new physics beyond the SM. The E821 experiment at Brookhaven National Lab (BNL) reported a 3.3σ deviation from the SM prediction that is written by [1–3]

$$\Delta a_\mu = a_\mu^{\exp} - a_\mu^{\rm SM} = (26.1 \pm 7.9) \times 10^{-10}. \quad (1.1)$$

Moreover a 3.7σ deviation was given by applying the lattice calculations as $\Delta a_\mu = (27.4 \pm 7.3) \times 10^{-10}$ in ref. [4] and $\Delta a_\mu = (27.06 \pm 7.26) \times 10^{-10}$ in Ref. [5]. Thus muon $g - 2$ is a long-standing anomaly in particle physics and various solutions have been considered; review can be found in [6–9]. Very recently the new muon $g - 2$ measurement in E989 experiment at Fermilab reported the new result indicating [10]

$$a_\mu^{\rm FNAL} = 116592040(54) \times 10^{-11}. \quad (1.2)$$

Combining BNL result we have new Δa_μ value of

*nomura@scu.edu.cn
†hiroshi.okada@apctp.org

$$\Delta a_\mu^{\rm new} = (25.1 \pm 5.9) \times 10^{-10}. \quad (1.3)$$

The deviation from the SM is now 4.2σ.

Experimental anomalies in rare B meson decays ($b \to s\ell\bar{\ell}$) also indicate deviation from the SM prediction. There are discrepancies in the measurements of the angular observable P_5' in the B meson decay ($B \to K^*\mu^+\mu^-$) [11–15], the lepton nonuniversality indicated by the ratio of branching fractions, $R_K = {\rm BR}(B^+ \to K^+\mu^+\mu^-)/{\rm BR}(B^+ \to K^+e^+e^-)$ [16–19], and $R_{K^*} = {\rm BR}(B \to K^*\mu^+\mu^-)/{\rm BR}(B \to K^*e^+e^-)$ [20]. Recently, the LHCb collaboration reported the updated result of R_K as [21]

$$R_K = 0.846^{+0.042+0.013}_{-0.039-0.012} \quad (1.1 {\rm ~GeV}^2 < q^2 < 6 {\rm ~GeV}^2),$$
$$(1.4)$$

where first(second) uncertainty is statical(systematic) one and q^2 is the invariant mass squared for dilepton. Remarkably the central value is the same as previous result [19] and we have 3.1σ deviation from the SM prediction. Motivated by these results, various global analysis for relevant Wilson coefficients are also carried out [22–26], which indicate negative contribution to Wilson coefficients C_9^μ and C_{10}^μ associated with $(\bar{s}_R\gamma^\mu b_L)(\bar{\mu}\gamma_\mu\mu)$ and $(\bar{s}_R\gamma^\mu b_L)(\bar{\mu}\gamma_\mu\gamma_5\mu)$ operators; global analyses with recent results including $B_s \to \mu^+\mu^-$ result by LHCb [21] is found in Refs. [26–29].

To explain the flavor issues above, one of the attractive scenarios is to introduce leptoquarks since they can interact with both leptons and quarks. In fact it is possible to explain muon $g - 2$ and/or $b \to s\ell\bar{\ell}$ anomalies by various leptoquark models [30–52]. We can obtain contribution to the Wilson coefficients $C_{9,10}^\mu$ for explaining

$b \to s\ell\bar{\ell}$ anomalies at tree level by introducing scalar leptoquarks with charge assignments $(\mathbf{3}, \mathbf{2}, 7/6)$ and $(\bar{\mathbf{3}}, \mathbf{3}, 1/3)$ under (SU(3), SU(2), U(1)) [30,33,36,38, 40,42,44,45,48–50]. In particular we can obtain different magnitude of C_9^μ and C_{10}^μ by combining these leptoquarks improving fit to the experimental data [33,42]. Moreover the leptoquark with charge $(\mathbf{3}, \mathbf{2}, 7/6)$ can provide sizable muon $g-2$ since it can couples to both left- and right-handed muon avoiding chiral suppression [40,42,49,50]. Yukawa interactions associated with some scalar leptoquarks can also generate active neutrino masses at loop level [38,39,41,43,50]. Remarkably we can realize neutrino mass by adding only two leptoquarks with charge assignments $(\mathbf{3}, \mathbf{2}, 1/6)$ and $(\bar{\mathbf{3}}, \mathbf{3}, 1/3)$ where we do not need any extra symmetry such as Z_2 [38]; note that other extra contents such as extra scalar fields and/or vectorlike fermions are required to generate radiative neutrino mass in other leptoquark combinations [39,41,43,50]. It is thus interesting to combine leptoquarks with charges $(\mathbf{3}, \mathbf{2}, 7/6)$, $(\bar{\mathbf{3}}, \mathbf{3}, 1/3)$, and $(\mathbf{3}, \mathbf{2}, 1/6)$ to explain $b \to s\ell\bar{\ell}$ anomalies, muon $g-2$, and neutrino mass.[1]

In this work we propose a model with three scalar leptoquarks. Combination of interactions among these leptoquarks and the SM fermions can explain muon $g-2$, $b \to s\ell\bar{\ell}$ anomaly and radiative neutrino mass generation at the same time. For neutrino mass generation, we adopt the mechanism in Ref. [38] realized by two leptoquarks, and one $SU(2)_L$ doublet leptoquark is added to improve $b \to s\ell\bar{\ell}$ explanation and to realize sizable muon $g-2$. We then analyze our model to find a solution to explain these issues taking into account possible flavor constraints such as lepton flavor violating (LFV) decays of charged leptons $(\ell \to \ell'\gamma)$ and mixing between meson and anti-meson (M–$\overline{M}$ mixing).

TABLE I. Charge assignments of the leptoquark fields η, η' and Δ under $SU(3)_C \times SU(2)_L \times U(1)_Y$.

	η	η'	Δ
$SU(3)_C$	$\mathbf{3}$	$\mathbf{3}$	$\bar{\mathbf{3}}$
$SU(2)_L$	$\mathbf{2}$	$\mathbf{2}$	$\mathbf{3}$
$U(1)_Y$	$\frac{1}{6}$	$\frac{7}{6}$	$\frac{1}{3}$

This paper is organized as follows. In Sec. II, we review our model and show relevant formulas for neutrino mass, Wilson coefficients for $b \to s\ell\bar{\ell}$ decay, LFV branching ratios(BRs), muon $g-2$ and M–$\overline{M}$ mixing for our analysis. In Sec. III, we carry out numerical analysis taking into account flavor constraints and show muon $g-2$ and Wilson coefficients which are compared with recent measurements (global fit results). We conclude in Sec. IV.

II. MODEL SETUP AND CONSTRAINTS

We review our model setup in this section. We introduce three types of leptoquark bosons η, η', and Δ. η has triplet under $SU(3)_C$, doublet under $SU(2)_L$, and 1/6 under $U(1)_Y$, and dominantly contributes to the neutrino masses. Δ has antitriplet under $SU(3)_C$, triplet under $SU(2)_L$, and 1/3 under $U(1)_Y$, and mainly contributes to the neutrino masses together with η, lepton anomalous magnetic moment, and lepton universality of $b \to s\mu\bar{\mu}$ both of which are recently reported that there could exist anomalies beyond the SM. η' has the same charges as η under $SU(3)_C$ and $SU(2)_L$, but 7/6 under $U(1)_Y$, and dominantly plays an role in suppressing the experimental bounds of $B \to \mu\bar{\mu}$ and BR($\mu \to e\gamma$).

The new field contents and their charges are shown in Table I. The relevant Lagrangian for the interactions of η and Δ with fermions and the Higgs field is given by

$$-\mathcal{L}_Y = f_{ij}\overline{d_{R_i}}\tilde{\eta}^\dagger L_{L_j} + g_{ij}\overline{Q^c_{L_i}}(i\sigma_2)\Delta L_{L_j} + h_{ij}\bar{Q}_{L_i}\eta'\ell_{R_j} + \tilde{h}_{ij}\bar{L}_{L_i}\tilde{\eta}'u_{R_j} + \text{H.c.}, \tag{2.1}$$

$$\mathcal{V}_{non-tri} = \mu H^\dagger \Delta\eta + \lambda_0 (H^T H)_{\mathbf{3}}[\eta'^\dagger\tilde{\eta}^*]_{\mathbf{3}} + \text{H.c.}, \tag{2.2}$$

where $(i, j) = 1$–3 are generation indices, $\tilde{\eta} \equiv i\sigma_2\eta^*$, σ_2 is the second Pauli matrix, and H is the SM Higgs field that develops a nonzero vacuum expectation value (VEV), which is denoted by $\langle H \rangle \equiv [0, v/\sqrt{2}]^T$. *Although λ_0 induces the mixing between $\eta_{2/3}$ and $\eta'_{2/3}$, we neglect this term for simplicity.* We work in the basis where all the coefficients are real and positive for simplicity.[2] The scalar fields can be parametrized as

$$H = \begin{bmatrix} w^+ \\ \frac{v+\phi+iz}{\sqrt{2}} \end{bmatrix}, \qquad \eta = \begin{bmatrix} \eta_{2/3} \\ \eta_{-1/3} \end{bmatrix}, \qquad \eta' = \begin{bmatrix} \eta'_{5/3} \\ \eta'_{2/3} \end{bmatrix}, \qquad \Delta = \begin{bmatrix} \frac{\delta_{1/3}}{\sqrt{2}} & \delta_{4/3} \\ \delta_{-2/3} & -\frac{\delta_{1/3}}{\sqrt{2}} \end{bmatrix}, \tag{2.3}$$

---

[1]In our previous work in Ref. [38] it is difficult to explain $b \to s\ell\bar{\ell}$ anomalies while fitting neutrino data and introduction of three leptoquarks is important.

[2]If we consider this mixing, it affects the neutrino masses, LFVs, muon $g-2$.

where the subscript of the fields represents the electric charge, $v \approx 246$ GeV, and $w^{\pm}$ and z are, respectively, the Nambu-Goldstone bosons, which are absorbed by the longitudinal components of the W and Z bosons. Due to the μ term in Eq. (2.2), the charged components with 1/3 and 2/3 electric charges mix each other, and their mixing matrices and mass eigenstates are defined as follows:

$$\begin{bmatrix} \eta_{i/3} \\ \delta_{i/3} \end{bmatrix} = O_i \begin{bmatrix} A_i \\ B_i \end{bmatrix}, \qquad O_i \equiv \begin{bmatrix} c_{\alpha_i} & s_{\alpha_i} \\ -s_{\alpha_i} & c_{\alpha_i} \end{bmatrix}, \quad (i = 1, 2), \tag{2.4}$$

where their mass eigenstates are denoted as m_{A_i} and m_{B_i}, respectively. Then the whole interaction in terms of the mass eigenstates can be written by

$$\begin{aligned}
-L_Y &\approx f_{ij}\overline{d_{R_i}}\nu_{L_j}(c_{\alpha_1}A_1 + s_{\alpha_1}B_1) - \frac{g_{ij}}{\sqrt{2}}\overline{d_{L_i}^c}\nu_{L_j}(-s_{\alpha_1}A_1 + c_{\alpha_1}B_1) \\
&\quad - f_{ij}\overline{d_{R_i}}\ell_{L_j}(c_{\alpha_2}A_2 + s_{\alpha_2}B_2) - \frac{g_{ij}}{\sqrt{2}}\overline{u_{L_i}^c}\ell_{L_j}(-s_{\alpha_1}A_1 + c_{\alpha_1}B_1) \\
&\quad - g_{ij}\overline{d_{L_i}^c}\ell_{L_j}\delta_{4/3} + g_{ij}\overline{u_{L_i}^c}\nu_{L_j}(-s_{\alpha_2}A_2^* + c_{\alpha_2}B_2^*) \\
&\quad + h_{ij}[\bar{u}_{Li}\ell_{Rj}\eta'_{5/3} + \bar{d}_{Li}\ell_{Rj}\eta'_{2/3}] + \tilde{h}_{ij}[\bar{\ell}_{Li}u_{Rj}\eta'_{-5/3} - \bar{\nu}_{Li}u_{Rj}\eta'_{-2/3}].
\end{aligned} \tag{2.5}$$

In the following we summarize various phenomenological formulas derived from these interactions.

A. Neutrino mixing

In our model active neutrino mass can be generated at one loop level via interactions among leptons, quarks and leptoquarks where the mechanism is the same as the one in Ref. [38]. Calculating one-loop diagram the active neutrino mass matrix m_ν is given by

$$(m_\nu)_{ab} = \sum_{i=1}^{3}[g_{bi}^T R_i f_{ia} + f_{ai}R_i g_{ib}^T],$$

$$R_i \approx -\frac{3s_{2\alpha_1}}{2(4\pi)^2}\ln\left(\frac{m_{A_1}}{m_{B_1}}\right)m_{d_i}, \tag{2.6}$$

where we assume $m_{d_i} \ll m_{A_1}, m_{B_1}$. $(m_\nu)_{ab}$ is diagonalized by the Pontecorvo-Maki-Nakagawa-Sakata mixing matrix $V_{\rm MNS}$ (PMNS) [53] as $(m_\nu)_{ab} = (V_{\rm MNS}D_\nu V_{\rm MNS}^T)_{ab}$ with $D_\nu \equiv (m_{\nu_1}, m_{\nu_2}, m_{\nu_3})$. Then, we rewrite g in terms of observables [54] and several input parameters as follows [38,55]:

$$g = \frac{1}{2}R^{-1}(f^T)^{-1}(V_{\rm MNS}D_\nu V_{\rm MNS}^T + A), \tag{2.7}$$

where A is an arbitrary three by three antisymmetric matrix with complex values, and perturbative limit $g \lesssim \sqrt{4\pi}$ has to be satisfied.

B. $b \to s\ell\bar{\ell}$

In our model $b \to s\ell\bar{\ell}$ can be induced by leptoquark exchanging process at tree level. The effective Hamiltonian to estimate the $b \to s\ell\bar{\ell}$ is given by

$$\begin{aligned}
H_{\rm eff} &= \frac{1}{2}\left(\frac{c_{\alpha_2}^2}{m_{A_2}^2} + \frac{s_{\alpha_2}^2}{m_{B_2}^2}\right)f_{2\ell}f_{\ell 3}^{\dagger}(\bar{s}\gamma_\mu P_R b)(\bar{\ell}\gamma^\mu P_L \ell) \\
&\quad - \frac{g_{2\ell}g_{\ell 3}^{\dagger}}{2m_{\delta_4}^2}(\bar{s}\gamma_\mu P_L b)(\bar{\ell}\gamma^\mu P_L \ell) \\
&\quad + \frac{h_{2\ell}h_{\ell 3}^{\dagger}}{2m_{\eta_2'}^2}(\bar{s}\gamma_\mu P_L b)(\bar{\ell}\gamma^\mu P_R \ell),
\end{aligned} \tag{2.8}$$

where m_{δ_4} and $m_{\eta_2'}$ are respectively the mass of $\delta_{4/3}$ and $\eta'_{2/3}$.

Then, we decompose Eq. (2.8) in terms of the effective operators $O_9^{(')}$ and $O_{10}^{(')}$ defined by $O_{9(10)} = \bar{s}\gamma_\mu P_L b\bar{\ell}\gamma^\mu(\gamma_5)\ell$, $O'_{9(10)} = \bar{s}\gamma_\mu P_R b\bar{\ell}\gamma^\mu(\gamma_5)\ell$, and their Wilson coefficients are found as

$$C_9^{LQ,\ell} = -\frac{1}{4c_{\rm SM}}\left(\frac{g_{2\ell}g_{\ell 3}^{\dagger}}{m_{\delta_4}^2} - \frac{h_{2\ell}h_{\ell 3}^{\dagger}}{m_{\eta_2'}^2}\right),$$

$$C_{10}^{LQ,\ell} = \frac{1}{4c_{\rm SM}}\left(\frac{g_{2\ell}g_{\ell 3}^{\dagger}}{m_{\delta_4}^2} + \frac{h_{2\ell}h_{\ell 3}^{\dagger}}{m_{\eta_2'}^2}\right), \tag{2.9}$$

$$C_9^{'LQ,\ell} = \frac{1}{4c_{\rm SM}}\left(\frac{c_{\alpha_2}^2}{m_{A_2}^2} + \frac{s_{\alpha_2}^2}{m_{B_2}^2}\right)f_{2\ell}f_{\ell 3}^{\dagger},$$

$$C_{10}^{'LQ,\ell} = -\frac{1}{4c_{\rm SM}}\left(\frac{c_{\alpha_2}^2}{m_{A_2}^2} + \frac{s_{\alpha_2}^2}{m_{B_2}^2}\right)f_{2\ell}f_{\ell 3}^{\dagger}, \tag{2.10}$$

where $c_{\rm SM} = V_{tb}V_{ts}^*\alpha G_F/(\sqrt{2}\pi)$ is a scale factor from the SM effective Hamiltonian. $C_{10}^{LQ,\mu}$ also contributes to $B_s \to \mu^+\mu^-$ whose experimental data is consistent with the SM prediction. In our numerical analysis we compare our

results with best fit values of these Wilson coefficients obtained from global fit [27] that includes all the B meson decay data. The best fit values for new physics contributions are

$$C_9^\mu = -0.91_{-0.17}^{+0.18}(-0.82_{-0.14}^{+0.14}) \quad \text{(for only } C_9\text{)}, \quad (2.11)$$

$$C_{10}^\mu = +0.51_{-0.24}^{+0.23}(+0.56_{-0.12}^{+0.12}) \quad \text{(for only} C_{10}\text{)}, \quad (2.12)$$

$$C_9^\mu = C_{10}^\mu = -0.41_{-0.15}^{+0.15}(-0.06_{-0.11}^{+0.11}), \quad (2.13)$$

$$C_9^\mu = -C_{10}^\mu - 0.65_{-0.12}^{+0.12}(-0.43_{-0.07}^{+0.07}), \quad (2.14)$$

$$\{C_9^\mu, C_{10}^\mu\} \simeq \{-0.67, 0.24\} \quad \text{(for } |C_9| \neq |C_{10}|$$
$$\text{for all rare } B \text{ decays)}, \quad (2.15)$$

where values outside(inside) bracket are for $b \to s\mu\bar{\mu}$ observables only (all rare B decays). Among them cases, only the cases with C_9^μ, $C_9^\mu = -C_{10}^\mu$ and $|C_9| \neq |C_{10}|$

improve fit more than 5σ compared to the SM case. On the other hand $C_9^\mu = C_{10}^\mu$ case less improve the fit.

C. LFVs and muon $g-2$

Yukawa interactions associated with leptoquarks induce LFV decay of $\ell \to \ell'\gamma$ at one-loop level. We then estimate the branching rations calculating relevant one-loop diagrams propagating leptoquarks. Branching ratio of $\ell_a \to \ell_b\gamma$ is given by

$$B(\ell_a \to \ell_b\gamma) = \frac{48\pi^3 C_{ab}\alpha_{\text{em}}}{G_F^2 m_a^2}(|(a_R)_{ab}|^2 + |(a_L)_{ab}|^2), \quad (2.16)$$

where $m_{a(b)}$ $(a(b) = 1, 2, 3)$ is the mass for the initial (final) eigenstate of charged-lepton; $1 \equiv e, 2 \equiv \mu, 3 \equiv \tau$, $(C_{21}, C_{31}, C_{32}) = (1, 0.1784, 0.1736)$. a_R is given by

$$(a_R)_{ab} \approx \frac{m_t}{(4\pi)^2} h_{3a}\tilde{h}_{b3}^\dagger \int_0^1 dx \int_0^{1-x} dy \left(\frac{5}{xm_t^2 + (1-y)m_{\eta_5'}^2} - \frac{2(1-x)}{xm_{\eta_5'}^2 + (1-y)m_t^2}\right)$$
$$+ \frac{m_c}{(4\pi)^2} h_{2a}\tilde{h}_{b2}^\dagger \int_0^1 dx \int_0^{1-x} dy \left(\frac{5}{xm_c^2 + (1-y)m_{\eta_5'}^2} - \frac{2(1-x)}{xm_{\eta_5'}^2 + (1-y)m_c^2}\right)$$
$$- \frac{g_{ia}g_{bi}^\dagger m_a}{8(4\pi)^2}\left(\frac{s_{\alpha_1}^2}{m_{A_1}^2} + \frac{c_{\alpha_1}^2}{m_{B_1}^2} - \frac{4}{m_{\delta_4}^2}\right) + \frac{3}{4(4\pi)^2}\left(\frac{h_{ia}h_{bi}^\dagger m_b}{m_{\eta_5'}^2} + \frac{\tilde{h}_{ia}^\dagger\tilde{h}_{bi}m_a}{m_{\eta_5'}^2}\right), \quad (2.17)$$

where m_t is the mass of top quark, and a_L is obtained by $m_a \leftrightarrow m_b$ in the last line. Clearly, the first term is dominant. The current experimental upper bounds are given by [56,57]

$$B(\mu \to e\gamma) \leq 4.2 \times 10^{-13}, \qquad B(\tau \to \mu\gamma) \leq 4.4 \times 10^{-8}, \qquad B(\tau \to e\gamma) \leq 3.3 \times 10^{-8}. \quad (2.18)$$

Our formula of the muon $g-2$ is given by

$$\Delta a_\mu \approx -m_\mu[(a_R)_{22} + (a_L)_{22}]. \quad (2.19)$$

We compare our value with the new result in Eq. (1.3).

D. Neutral meson mixings $M - \overline{M}$

Mixings between meson and antimeson are induced by box diagrams propagating leptoquarks. We have to estimate the mixings, since $M - \overline{M}$ mixings $(M = K_0(d\bar{s}), B_d(d\bar{b}), B_s(s\bar{b}), D_0(c\bar{u}))$, are precisely measured and there exist strong constraints. This estimation can be achieved by effective operators [58], and each of their formulas is given by

$$\Delta m_{M_d} \approx -\frac{m_{M_d}f_{M_d}^2}{6(4\pi)^2} \sum_{a,}^3 \sum_{a'=1} \left(\text{Re}[f_{ja}f_{ai}^\dagger f_{ka'}f_{a'\ell}^\dagger]\left[\sum_{q=1,2}\left(\frac{c_{\alpha_q}^2}{m_{A_q}^2} + \frac{s_{\alpha_q}^2}{m_{B_q}^2} + 4s_{\alpha_q}c_{\alpha_q}F_M(A_q, B_q)\right)\right]\right.$$
$$+ \frac{1}{4}\text{Re}[g_{aj}^\dagger g_{ia}g_{a'k}^\dagger g_{\ell a'}]\left[\frac{s_{\alpha_1}^2}{m_{A_1}^2} + \frac{c_{\alpha_1}^2}{m_{B_1}^2} - 4s_{\alpha_1}c_{\alpha_1}F_M(A_1, B_1) + \frac{4}{m_{\delta_4}^2}\right]$$
$$+ \frac{1}{m_{\eta_2'}^2}[\text{Re}[h_{ja}h_{ai}^\dagger h_{ka'}h_{a'\ell}^\dagger] + \text{Re}[\tilde{h}_{ja}^\dagger\tilde{h}_{ai}\tilde{h}_{ka'}^\dagger\tilde{h}_{a'\ell}]]), \quad (2.20)$$

$$\Delta m_{M_u} \approx -\frac{m_{M_u} f^u_{M_d}}{6(4\pi)^2} \sum_{a,a'=1}^{3} \left(\frac{1}{4} \text{Re}[g^\dagger_{aj} g_{ia} g^\dagger_{a'k} g_{\ell a'}] \left[\sum_{q=1,2} q^2 \left(\frac{s^2_{\alpha_q}}{m^2_{A_q}} + \frac{c^2_{\alpha_q}}{m^2_{B_q}} - 4 s_{\alpha_q} c_{\alpha_q} F_M(A_q, B_q) \right) \right] \right.$$

$$\left. + \frac{1}{m^2_{\eta'_5}} [\text{Re}[h_{ja} h^\dagger_{ai} h_{ka'} h^\dagger_{a'\ell}] + \text{Re}[\tilde{h}^\dagger_{ja} \tilde{h}_{ai} \tilde{h}^\dagger_{ka'} \tilde{h}_{a'\ell}]] \right), \tag{2.21}$$

where $F_M(m_1, m_2)$ is given by

$$F_M(m_1, m_2) = \int_0^1 dx \int_0^{1-x} dy \frac{1-x-y}{xm_1^2 + ym_2^2}. \tag{2.22}$$

The current constraints are found as follows [3,59]:

$$\Delta m_{M_d}[(ijk\ell) = (1221)], \qquad \Delta m_K \lesssim 3.48 \times 10^{-15} \text{ [GeV]}, \tag{2.23}$$

$$\Delta m_{M_d}[(ijk\ell) = (1331)], \qquad -1.85 \times 10^{-13} \text{ [GeV]} \lesssim \Delta m_{B_d} \lesssim 4.05 \times 10^{-14} \text{ [GeV]}, \tag{2.24}$$

$$\Delta m_{M_d}[(ijk\ell) = (2332)], \qquad -2.77 \times 10^{-12} \text{ [GeV]} \lesssim \Delta m_{B_s} \lesssim 1.07 \times 10^{-12} \text{ [GeV]}, \tag{2.25}$$

$$\Delta m_{M_u}[(ijk\ell) = (2112)], \qquad \Delta m_D \lesssim 6.25 \times 10^{-15} \text{ [GeV]}, \tag{2.26}$$

where we apply the following values in our analysis: $f_K \approx 0.156$ GeV, $f_{B_d(B_s)} \approx 0.191(0.274)$ GeV [60,61], $f_D \approx 0.212$ GeV, $m_K \approx 0.498$ GeV, $m_{B_d(B_s)} \approx 5.280(5.367)$ GeV, and $m_D \approx 1.865$ GeV.

III. NUMERICAL ANALYSIS

In this section, we carry out numerical analysis scanning free parameters of the model searching for solutions to fit neutrino oscillation data and to explain B anomalies and muon $g - 2$, taking into account all the flavor constraints discussed above. First, we assume almost degenerate leptoquark masses $M_{LQ} \equiv m_{\delta4} = m_{\eta'_{2.5}} = m_{A_{1,2}} = m_{B_2}$ for simplicity; we only take $m_{B_2} = M_{LQ} \pm 10$ GeV to avoid too small R_i in Eq. (2.6). In fact degeneracy of masses for the components of $\eta^{(')}$ and Δ is motivated to suppress the oblique S- and T-parameters.[3] We then scan our parameters with the following ranges:

$$M_{LQ} \in [1, 5] \text{ TeV}, \quad |A_{12,23,13}| \in [10^{-13}, 10^{-7}] \text{ GeV}, \quad (\alpha_1, \alpha_2) \in [10^{-5}, 10^{-2}],$$

$$|f_{ij}| \in [10^{-7}, 10^{-3}], \quad \{|h_{1i}|, |h_{i1}|\} \in [10^{-7}, 10^{-3}], \quad |h_{ab}(a, b \neq 1)| \in [10^{-5}, \sqrt{4\pi}],$$

$$\{|\tilde{h}_{1i}|, |\tilde{h}_{i1}|\} \in [10^{-7}, 10^{-3}], \quad |\tilde{h}_{ab}(a, b \neq 1)| \in [10^{-5}, \sqrt{4\pi}]. \tag{3.1}$$

Here we choose smaller values of Yukawa coupling associated with first generation to avoid strong flavor constraints. The Yukawa couplings g_{ij} are obtained from Eq. (2.7) to fit neutrino oscillation data. Note that we select smaller values for Yukawa coupling f_{ij} so that g_{ij} can be sizable to fit neutrino data. As a result $C'^{LQ,\ell}_{9,10}$ is suppressed and we do not show these values explicitly. Then we impose constraints from BR($\ell \to \ell'\gamma$) and $M-\overline{M}$ mixing discussed in previous section, and obtain the possible values of Wilson coefficient $C^{LQ,\mu}_{9,10}$ and Δa_μ for allowed parameter sets.

In Fig. 1, we show our results for $C^{LQ,\mu}_9$ and $C^{LQ,\mu}_{10}$ values where we impose $\Delta a_\mu > 0$ in addition to the other constraints. We find that many parameter sets give $C^{LQ,\mu}_9 \sim \pm C^{LQ,\mu}_{10}$. Note that we have less points for same sign case $C^{LQ,\mu}_9 \sim C^{LQ,\mu}_{10}$ compared to opposite sign case since same sign contribution comes from Yukawa coupling g that is more constrained by neutrino data. Although some tunings of parameters are required, we can obtain the case of $|C^{LQ,\mu}_{10}| \neq |C^{LQ,\mu}_9|$ due to cancellation between diagrams. Thus we have more freedom to obtain $\{C_9, C_{10}\}$ values thanks to the contributions from two different leptoquarks. In principle we can obtain all the best fit values in Ref. [27] summarized by Eqs. (2.11)–(2.15) and that for $C^{LQ,\mu}_9 = -C^{LQ,\mu}_{10}$ case can be most easily realized.
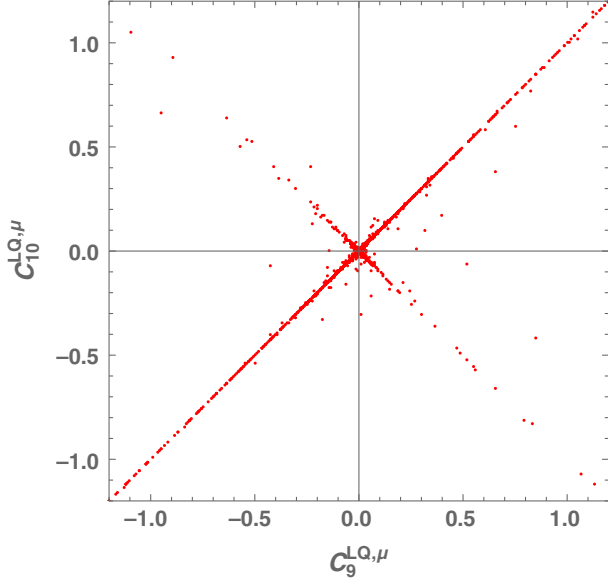
---

[3]We thus do not explicitly consider these oblique parameters making them to be small by degenerate masses.

FIG. 1. ΔC_9^μ and ΔC_{10}^μ values for parameter sets satisfying neutrino data and all flavor constraints. The shaded area indicates new muon $g - 2$ value in Eq. (1.3).

In Fig. 2, we show the values of $C_{9(10)}^{LQ,\mu}$ and Δa_μ that is compared with the new muon $g - 2$ result Eq. (1.3) in the left(right) figure. As we see, it is possible to obtain the observed value of muon $g - 2$ and $C_9^{LQ,\mu} \sim -1$ at the same time; we also find both sign of $C_{10}^{LQ,\mu}$ is achieved. Note that sizable contribution is obtained due to enhancement by m_t in Eq. (2.17). Therefore we have parameter sets which explain both $b \to s\ell\bar{\ell}$ and muon $g - 2$ anomalies. Note that we do not find clear dependence on LQ masses and any values in [1.0, 5.0] TeV are allowed.

IV. CONCLUSIONS

We have discussed a model with three leptoquarks $\{\Delta, \eta, \eta'\}$ to explain $b \to s\ell\bar{\ell}$ anomalies, muon $g - 2$ and neutrino masses, motivated by recent experimental results. Active neutrino mass is generated at one-loop level via interactions among Δ, η and SM fermions. The leptoquarks Δ and η' contribute to Wilson coefficient $C_{9,10}^\ell$ at tree level. Interestingly combination of two leptoquark contributions can provide a case of $|C_9^{LQ,\mu}| \neq |C_{10}^{LQ,\mu}|$ in contrast to one leptquark scenario. In addition all three leptoquarks can provide contribution to muon $g - 2$, and induce LFV decay processes and M–$\bar{M}$ mixing which are taken into account as constraints. We then have carried out numerical analysis to explore $C_{9,10}^{LQ,\mu}$ and muon $g - 2$ values when neutrino data and relevant flavor constraints are accommodated. Our findings are as follows:

(1) We can obtain sizable muon $g - 2$ from η' loop due to m_t enhancement. Then we can fit the value of the new muon $g - 2$ result shown in Eq. (1.3).

(2) $C_9^{LQ,\mu} = -C_{10}^{LQ,\mu}$ case is preferred in our scenario but we can obtain $|C_9^{LQ,\mu}| \neq |C_{10}^{LQ,\mu}|$ case due to contributions from two leptoquarks. It is thus possible to obtain the best fit values from global analysis not only for $C_9^{LQ,\mu} = -C_{10}^{LQ,\mu}$. In addition we can accommodate explanation of $b \to s\ell\bar{\ell}$ and muon $g - 2$ at the same time.

(3) Leptoquark masses are not constrained if they are TeV scale. The collider experiments would constrain the mass range in future.

Thus combination of leptoquarks is attractive scenario to explain $b \to s\ell\ell$ anomaly, muon $g - 2$ and neutrino mass at the same time.

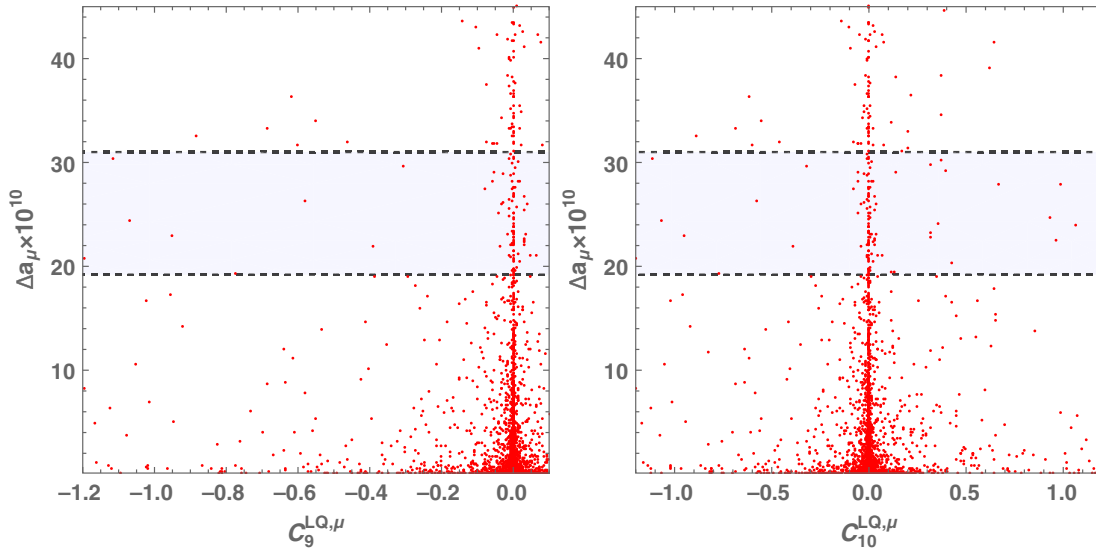FIG. 2. $C_{9(10)}^{LQ,\mu}$ and Δa_μ values for parameter sets satisfying neutrino data and all flavor constraints in the left(right) side figure.

ACKNOWLEDGMENTS

[1] G. W. Bennett *et al.* (Muon g-2 Collaboration), Phys. Rev. D **73,** 072003 (2006).

[2] M. Davier, A. Hoecker, B. Malaescu, and Z. Zhang, Eur. Phys. J. C **80,** 241 (2020); **80,** 410(E) (2020).

[3] P. A. Zyla *et al.* (Particle Data Group), Prog. Theor. Exp. Phys. **2020,** 083C01 (2020).

[4] T. Blum, P. A. Boyle, V. Gülpers, T. Izubuchi, L. Jin, C. Jung, A. Jüttner, C. Lehner, A. Portelli, and J. T. Tsang (RBC and UKQCD Collaborations), Phys. Rev. Lett. **121,** 022003 (2018).

[5] A. Keshavarzi, D. Nomura, and T. Teubner, Phys. Rev. D **97,** 114025 (2018).

[6] F. Jegerlehner and A. Nyffeler, Phys. Rep. **477,** 1 (2009).

[7] J. P. Miller, E. de Rafael, B. L. Roberts, and D. Stockinger, Annu. Rev. Nucl. Part. Sci. **62,** 237 (2012).

[8] M. Lindner, M. Platscher, and F. S. Queiroz, Phys. Rep. **731,** 1 (2018).

[9] F. Jegerlehner, Acta Phys. Pol. B **49,** 1157 (2018).

[10] B. Abi *et al.* (Muon g-2 Collaboration), Phys. Rev. Lett. **126,** 141801 (2021).

[11] S. Descotes-Genon, J. Matias, M. Ramon, and J. Virto, J. High Energy Phys. 01 (2013) 048.

[12] R. Aaij *et al.* (LHCb Collaboration), J. High Energy Phys. 02 (2016) 104.

[13] R. Aaij *et al.* (LHCb Collaboration), Phys. Rev. Lett. **111,** 191801 (2013).

[14] A. Abdesselam *et al.* (Belle Collaboration), arXiv:1604.04042.

[15] S. Wehle *et al.* (Belle Collaboration), Phys. Rev. Lett. **118,** 111801 (2017).

[16] G. Hiller and F. Kruger, Phys. Rev. D **69,** 074020 (2004).

[17] C. Bobeth, G. Hiller, and G. Piranishvili, J. High Energy Phys. 12 (2007) 040.

[18] R. Aaij *et al.* (LHCb Collaboration), Phys. Rev. Lett. **113,** 151601 (2014).

[19] R. Aaij *et al.* (LHCb Collaboration), Phys. Rev. Lett. **122,** 191801 (2019).

[20] R. Aaij *et al.* (LHCb Collaboration), J. High Energy Phys. 08 (2017) 055.

[21] R. Aaij *et al.* (LHCb Collaboration), arXiv:2103.11769.

[22] S. Descotes-Genon, L. Hofer, J. Matias, and J. Virto, J. High Energy Phys. 06 (2016) 092.

[23] M. Ciuchini, A. M. Coutinho, M. Fedele, E. Franco, A. Paul, L. Silvestrini, and M. Valli, Eur. Phys. J. C **79,** 719 (2019).

[24] M. Algueró, B. Capdevila, A. Crivellin, S. Descotes-Genon, P. Masjuan, J. Matias, and J. Virto, Eur. Phys. J. C **79,** 714 (2019).

[25] J. Aebischer, W. Altmannshofer, D. Guadagnoli, M. Reboud, P. Stangl, and D. M. Straub, Eur. Phys. J. C **80,** 252 (2020).

[26] A. K. Alok, A. Dighe, S. Gangal, and D. Kumar, J. High Energy Phys. 06 (2019) 089.

[27] W. Altmannshofer and P. Stangl, arXiv:2103.13370.

[28] C. Cornella, D. A. Faroughy, J. Fuentes-Martín, G. Isidori, and M. Neubert, arXiv:2103.16558.

[29] J. Kriewald, C. Hati, J. Orloff, and A. M. Teixeira, arXiv:2104.00015.

[30] S. Sahoo and R. Mohanta, Phys. Rev. D **91,** 094019 (2015).

[31] S. Sahoo and R. Mohanta, New J. Phys. **18,** 013032 (2016).

[32] M. Bauer and M. Neubert, Phys. Rev. Lett. **116,** 141802 (2016).

[33] C. H. Chen, T. Nomura, and H. Okada, Phys. Rev. D **94,** 115005 (2016).

[34] D. Becirevic, S. Fajfer, N. Kosnik, and O. Sumensari, Phys. Rev. D **94,** 115021 (2016).

[35] S. Sahoo, R. Mohanta, and A. K. Giri, Phys. Rev. D **95,** 035027 (2017).

[36] D. Becirevic, N. Kosnik, O. Sumensari, and R. Z. Funchal, J. High Energy Phys. 11 (2016) 035.

[37] G. Hiller, D. Loose, and K. Schönwald, J. High Energy Phys. 12 (2016) 027.

[38] K. Cheung, T. Nomura, and H. Okada, Phys. Rev. D **94,** 115024 (2016).

[39] O. Popov and G. A. White, Nucl. Phys. **B923,** 324 (2017).

[40] E. C. Leskow, A. Crivellin, G. D'Ambrosio, and D. Muller, Phys. Rev. D **95,** 055018 (2017).

[41] K. Cheung, T. Nomura, and H. Okada, Phys. Lett. B **768,** 359 (2017).

[42] C. H. Chen, T. Nomura, and H. Okada, Phys. Lett. B **774,** 456 (2017).

[43] Y. Cai, J. Gargalionis, M. A. Schmidt, and R. R. Volkas, J. High Energy Phys. 10 (2017) 047.

[44] P. Arnan, D. Becirevic, F. Mescia, and O. Sumensari, J. High Energy Phys. 02 (2019) 109.

[45] O. Popov, M. A. Schmidt, and G. White, Phys. Rev. D **100,** 035028 (2019).

[46] A. Datta, J. L. Feng, S. Kamali, and J. Kumar, Phys. Rev. D **101,** 035010 (2020).

[47] I. Doršner, S. Fajfer, and O. Sumensari, J. High Energy Phys. 06 (2020) 089.

[48] A. Crivellin, D. Müller, and F. Saturnino, J. High Energy Phys. 06 (2020) 020.

[49] A. Crivellin, D. Mueller, and F. Saturnino, arXiv:2008.02643.

[50] K. S. Babu, P. S. B. Dev, S. Jana, and A. Thapa, J. High Energy Phys. 03 (2021) 179.

[51] A. Angelescu, D. Bečirević, D. A. Faroughy, F. Jaffredo, and O. Sumensari, arXiv:2103.12504.

[52] A. Greljo, P. Stangl, and A. E. Thomsen, arXiv:2103.13991.

[53] Z. Maki, M. Nakagawa, and S. Sakata, Prog. Theor. Phys. **28**, 870 (1962).

[54] I. Esteban, M. C. Gonzalez-Garcia, M. Maltoni, T. Schwetz, and A. Zhou, J. High Energy Phys. 09 (2020) 178; NuFIT 5.0 (2020), www.nu-fit.org.

[55] T. Nomura and H. Okada, Phys. Rev. D **94**, 093006 (2016).

[56] A. M. Baldini *et al.* (MEG Collaboration), arXiv:1605 .05081.

[57] J. Adam *et al.* (MEG Collaboration), Phys. Rev. Lett. **110**, 201801 (2013).

[58] F. Gabbiani, E. Gabrielli, A. Masiero, and L. Silvestrini, Nucl. Phys. **B477**, 321 (1996).

[59] N. Kumar, T. Nomura, and H. Okada, arXiv:2002.12218.

[60] L. Di Luzio, M. Kirk, and A. Lenz, Phys. Rev. D **97**, 095035 (2018).

[61] L. Di Luzio, M. Kirk, and A. Lenz, arXiv:1811.12884.